

Bootstrap energization of relativistic electrons in magnetized plasmas

Ilan Roth

Space Sciences, University of California at Berkeley, Berkeley, CA 94720, USA
email: ilan@ssl.berkeley.edu

Abstract. *In situ* and remote observations indicate that relativistic or ultra relativistic electrons are formed at various magnetized configurations. It is suggested that a specific bootstrap mechanism operates in some of these environments. The mechanism applies to (a) relativistic electrons observed on localized field lines in outer radiation belt - through a process initiated at a distant substorm injection; (b) relativistic electrons observed at the interplanetary medium - through a process initiated via coronal injection, at large distances from flares or propagating CME; (c) ultra-relativistic electrons deduced at the galactic jets - through a process initiated via local injection at the small-scale magnetic field. The injected nonisotropic electrons excite whistler waves which boost efficiently the tail of the electron distribution.

Keywords. acceleration of particles, plasmas, jets, radiation mechanisms: nonthermal

1. Introduction

Direct *in situ* heliospheric measurements on board spacecraft and remote solar, heliospheric and astrophysical observations through electromagnetic emissions indicate that energization mechanisms of electron populations to quasi-relativistic, relativistic or ultra-relativistic energies operate at various magnetized plasmas. The *in situ* measurements relate principally to enhanced fluxes of relativistic electrons (i) in the terrestrial outer radiation belts at $L \sim 4-10$ (denoting equatorial distance of a dipole-like field in units of Earth radius), and (ii) at the interplanetary medium, mainly at heliospheric distances of ~ 1 AU, capturing electrons of solar origin. The magnetospheric enhancements of relativistic electrons coincide with the recovery phase of geomagnetic storms and possibly with sub-storm injections, while the relation of the relativistic heliospheric electrons to flares or to Coronal Mass Injections (CMEs) shocks still remains debatable. Remote solar and heliospheric electromagnetic observations at various wavelengths reveal the energy spectra of the non-thermal electrons, the locations of the emission processes and together with the *in-situ* measurements impose constraints on the energization mechanisms. The fluxes of (ultra)relativistic electrons of astrophysical origin are remotely deduced through observation of radiative emissions. Some of the most intense occurrences of these electromagnetic waves are related to jets emanating from accretion discs in radio active galactic nuclei. Although all these observations relate to vastly different magnetized plasmas with various geometries, the question rises regarding a possibility that similar processes operate in these environments.

It is conjectured, therefore, that an analogous physical process at various magnetic configurations may enhance a subset of relativistic electron fluxes in magnetospheric, solar, and astrophysical jet plasmas. The bootstrap mechanism requires existence of a stressed, large-scale magnetic structure, distant injection of seed non-isotropic

electrons due to reconnection and energization on closed, inhomogeneous magnetic fields lines.

2. Overview

Electrons form excellent tracers of magnetic field and an important source of electromagnetic radiation: coherent emissions due to collective plasma processes and incoherent single particle emissions due to interaction with plasma or with magnetic field.

a) Terrestrial (planetary) magnetic storms are initiated by an intense, persistent southward interplanetary field which deforms the geomagnetic field, increasing the ring current and decreasing the energetic electron population in the radiation belt (Fig. 1a). In the storm recovery phase the fluxes of relativistic electrons increase often by orders of magnitude above the pre-storm level over few days as a result of Ultra Low Frequency waves diffusion across the actively distorted magnetospheric fields, towards lower L shells (stronger magnetic field), by preserving the first adiabatic invariant and increasing the energy (Baker *et al.*, 1986; Reeves *et al.*, 2003); however, many satellite crossings observe fast (~ 1 hour) and large enhancement with a peak at $L \sim 4.0$, indicating local energization at a confined region of field lines. Various observations (Meredith *et al.*, 2003) correlate this enhancement with the observed substorm injection of sub-relativistic, non isotropic electrons and excitation of magnetospherically reflected whistler waves along the inhomogeneous field lines (Bortnik *et al.*, 2006, Shklyar *et al.*, 2004). The interaction between whistler waves and electrons extends the tail of the distribution into the relativistic domain. Therefore, the observed peaks of relativistic electron fluxes at low L-shells are formed by a bootstrap process initiated via distant injection at large L shells.

b) Solar flares are initiated due to a reconfiguration of the magnetically unstable coronal field, with ensuing injection of electron and ion fluxes towards the chromosphere, exciting emissions at radio, X-ray and γ -ray frequencies. Additionally, magnetic stress release may result in a detachment of a large blob of plasma ($\sim 10^{15}$ g) and its propulsion into the interplanetary medium in the form of Coronal Mass Ejections (CME; Fig 1b). Type III bursts are observed when an electron beam propagates along magnetic field and excites Langmuir waves at the local plasma frequency, which are then partially converted into coherent electromagnetic radiation (Lin, 1985, Wang *et al.*, 2006). The Langmuir waves indicate the local density, allowing one to determine the coronal or interplanetary excitation locations and the beam propagation speed. Type II emissions reflect the location of the propagating CME shock. Precise timing of the observed electron fluxes at ~ 1 AU (Krucker *et al.*, 1999) showed that one may distinguish between low-energy electrons (< 20 keV) which are injected almost instantaneously with the type III emission and more energetic electrons with a delay of 10-30 minutes. Similarly, mildly relativistic fluxes at 30-350 keV were delayed by up to 40 minutes with respect to the metric type-III, hard X rays and microwave electromagnetic emissions (Haggerty *et al.*, 2003). Long-lasting relativistic electron fluxes, which are observed in conjunction with flares (X rays and type III) and intense CMEs (type II emissions) show an onset of 25 minutes after the type III initialization (Klassen *et al.*, 2005), while Nancay Radioheliograph observations correlate these relativistic enhancements to coronal bursts of 100-s MHz emissions, without connectivity to the flare site and behind the intense CME (Maia *et al.*, 2004; Pick *et al.*, 2005). Hence, these bursts release magnetic energy in the CME evacuated domain in the form of subrelativistic seed electrons, which, in analogy to terrestrial substorms or lightnings, excite whistlers that extend the electron tail into relativistic energies (Roth, 2008). Therefore, the observed delayed relativistic electrons in the interplanetary medium

are energized through a bootstrap process initiated via coronal injection, on closed field lines, at large distances from the flare sites or/and CME shock.

c) An active galactic nucleus is a compact region at the center of a galaxy with an unusually high luminosity powered by accretion onto massive black hole; in these accretion discs the conversion of the gravitational to radiation energy can reach the Eddington luminosity limit. Some accretion discs produce highly collimated and fast outflowing jets, whose formation mechanism is not fully understood but believed to result due to acceleration and squeezing of plasma by a twisting magnetic field (Blandford and Payne, 1982; Fendt and Memola, 2001). These relativistic jets extend as far as tens/hundreds of kilo-parsecs from the central black hole (Fig 1c) and are known to provide electrons with a huge relativistic factor up to $\gamma \sim 10^6$. They exhibit obvious observational effects in the radio waveband, where Very Large Array, Hubble Space Telescope and Chandra X-ray Observatory can be used to study the radiation they emit down to sub-parsec scales. Two correlated problems of jet emission include (i) confirmation of the radiation process and (ii) long-duration of its energetic source. The main emission mode is (Lorentz boosted) synchrotron and the observed cutoff (due to the progressive emission softening with increasing energy) is attributed to a cooling process of a single source electron population in a large scale magnetic field (Meisenheimer and Heavens, 1986), with a time scale much shorter than the temporal extent of the jets, which necessitates continuous replenishment of the energetic electrons. Additionally, several recent measurements at a very high resolution of 0.3 arcsec (Jester *et al.*, 2005) indicate flattening of the UV spectrum, requiring either second electron component or a different emission process. An elegant solution for this flattening stipulates that a significant part of the magnetic energy density exists in the form of inhomogeneous, small-scale magnetic fields such that electron trajectory is distorted from a simple gyration through interaction with random small-scale fields, resulting in a "jitter" emission (Medvedev, 2000) and in flattening of the spectrum through diffusive synchrotron radiation (Fleishman, 2006). Simulations of similar configurations indicate formation of these small scale structures (Frederiksen *et al.*, 2004; Nishikawa *et al.*, 2005) far behind the shock. It is conjectured that the adjacent, marginally stable, reconnecting small-scale magnetic field arcs inject a seed of non-isotropic electrons into the closed field lines, analogously to the solar scenario, and through efficient resonant interactions with whistlers the tail of the electron distribution is boosted to ultra relativistic energies. Therefore, the ultra-relativistic jet electrons are energized through a bootstrap process initiated via local injection at the small-scale magnetic field.

3. The Bootstrap model

The above-described configurations and processes feature several similarities, in spite of significant differences in the magnetic geometry and in energization time scales. In all of the configurations there exists directly measurable or indirectly deduced large-scale,

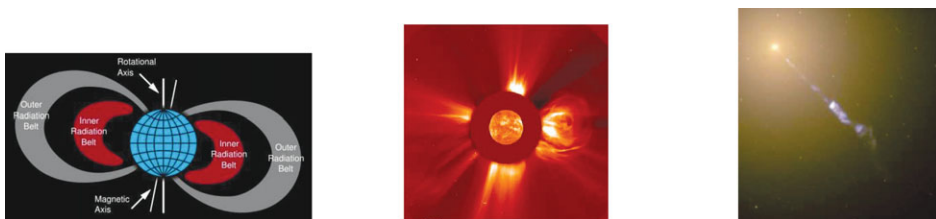


Figure 1. (a) Sketch of the terrestrial radiation belts. (b) Imaged solar corona with an uplifting CME (LASCO). (c) Jet from Galaxy M87 (Hubble Heritage Project).

deformed field and additional marginally stable field configuration which injects non-isotropic electron populations into closed magnetic fields. These electrons excite whistler waves which propagate and reflect along the magnetic field lines boosting efficiently the energetic tail of the distribution.

3.1. Wave propagation

The nonisotropic distribution of the injected electrons constitutes a source of propagating waves with group velocity directed mainly along the magnetic field. The main excited mode is whistler; its phase/group velocities and amplitude depend on the electron pitch angle distribution and the local plasma parameters.

Oblique whistler eigenmode with wavenumber $\mathbf{k} = (k_{\perp}, k_{\parallel}) = (k \sin\theta, 0, k \cos\theta)$ and frequency ω , propagating at an angle $\theta = \cos^{-1}(k_{\parallel}/k)$ with respect to the magnetic field is supported by the bulk of injected electrons; neglecting thermal and relativistic effects (justified for the terrestrial and solar injections while requiring correction for more energetic jet injection), the local dispersion relation, with negligible gradients, becomes:

$$(kc/\omega)^2 = [B + (B^2 - 4AC)^{1/2}]/2A \quad (3.1)$$

where $A = \epsilon_1 \sin^2\theta + \epsilon_3 \cos^2\theta$, $B = \epsilon_1 (\epsilon_3 + A) - \epsilon_2^2 \sin^2\theta$, $C = \epsilon_3 (\epsilon_1^2 - \epsilon_2^2)$, while ϵ_i denote the components of the dielectric tensor. For parallel propagation ($\theta = 0$), neglecting the ions, Eq (3.1) degenerates into $(kc/\omega)^2 = 1 + \omega_e^2/[(\Omega - \omega)\omega]$, where ω_e and Ω denote the plasma and the nonrelativistic gyrofrequency of the injected electrons, respectively. Whistler ray propagating along an inhomogeneous magnetic field may undergo reflection when its wave normal passes through $\pi/2$ and its longitudinal group velocity $V_{g\parallel}$ reverses sign (e.g., Kimura, 1966, 1985). Hence, this reflecting wave, as observed by numerous satellites, may resonate with bouncing particles numerous times.

3.2. Resonant interaction

Over short interaction times between electrons with gyroradius $\rho = \gamma v_{\perp}/\Omega$ and gyrofrequency Ω/γ (γ denotes the relativistic factor) and whistler waves, when the plasma and wave parameters change slowly, irreversible changes in energy, adiabatic invariant and pitch angle may take place. Direct integration of the unperturbed trajectories ($z = v_{\parallel}t, x = \rho \sin(\Omega t/\gamma)$) in the propagating wave frame gives

$$\cos(k_{\parallel}z + k_{\perp}x - \omega t) \sim \Sigma J_n(k_{\perp}\rho) \cos[k_{\parallel}v_{\parallel}t - (\omega - n\Omega/\gamma)t] \quad (3.2)$$

indicating that as an electron and a whistler propagate along the magnetic field, they may encounter numerous locations where the phase is almost stationary, resulting in the resonance condition (for an integer n)

$$k_{\parallel}v_{\parallel} = \omega - n\Omega/\gamma. \quad (3.3)$$

For finite $k_{\perp}\rho$ all regular $n < 0$ and anomalous $n > 0$ harmonics contribute to changes in energy and pitch angles. Bessel function J_n in (3.2) signifies the increased interaction effectiveness with a higher electron energy. Hence, if the phase angle ζ between the perpendicular electric wave field E_{\perp} and velocity is hardly modified during the interaction time, while the parallel velocity satisfies (3.3), the electron undergoes an irreversible energy change

$$d\gamma/dt \sim (e/mc^2) E_{\perp} v_{\perp} \sin\zeta \quad (3.4)$$

Electron dynamics with a monochromatic (3.2) whistler wave may be analyzed through the normalized relativistic Hamiltonian $H(\mathbf{x}, \mathbf{P})$ with $\mathbf{P} = m\mathbf{v}\gamma + q\mathbf{A}(\mathbf{x})/c$ and (3.2):

$$H = [1 + (\mathbf{p} - \mathbf{A}(\mathbf{x}))^2]^{1/2} + \Phi(\mathbf{x}) \quad (3.5)$$

where the canonical momentum \mathbf{P} is normalized to mc , the time t to the inverse gyrofrequency at the reference position Ω_o^{-1} , the spatial coordinates \mathbf{x} to c/Ω_o , and the wavenumber k to Ω_o/c . The background magnetic field is represented by the normalized potential $\mathbf{A}_o = x\eta(\delta z)\mathbf{y}$, with the normalized gyrofrequency $\eta(\delta z) = \Omega(\delta z)/\Omega_o$, where the δ dependence denotes the slowly changing gyrofrequency (mirror force). The wave electric field $[E_x \cos \psi, E_y \sin \psi, E_z \cos \psi]$ is derived from the electrostatic $\Phi = \delta_o \sin \psi$ and the electromagnetic potential $\mathbf{A} = [\delta_1(k_{\parallel}/k) \sin \psi, \delta_2 \cos \psi, -\delta_1(k_{\perp}/k) \sin \psi]$, with the phase $\psi = [\int \mathbf{k}(\delta z) \cdot \mathbf{x} - \omega t]$. Two canonical transformations cast the equations of motion around a single resonance into (Roth *et al.*, 1999)

$$dZ/dt \sim [(P_{\parallel} + l\eta/k_{\parallel})/\gamma_o - \omega/k_{\parallel}] + (\partial G_l/\partial P_{\parallel}) \cos(k_{\parallel}Z)/k_{\parallel} \tag{3.6}$$

$$dP_{\parallel}/dt = -(I/\gamma_o)(\partial\eta/\partial z) + G_l k_{\parallel} \sin(k_{\parallel}Z) \tag{3.7}$$

where $Z = z + l\theta/k_{\parallel} - \pi/2k_{\parallel} - (\omega/k_{\parallel})t$, $I = I' + lP_{\parallel}/k_{\parallel}$, and

$$G_l = [\delta_1(P_{\parallel} \sin\phi - l \eta \cos\phi/k_{\perp})/\gamma_o + \delta_o] J_l[k_{\perp} \sqrt{2I/\eta}] + \delta_2[\sqrt{2I\eta/\gamma_o}] J_l'[k_{\perp} \sqrt{(2I/\eta)}] \tag{3.8}$$

The G_l terms describe higher harmonic coupling while a negligible stationary phase $k_{\parallel}Z$ (similarly to (3.2)) satisfies the resonance condition (first term of 3.6) and assures small parallel acceleration (3.7); I' is an adiabatic invariant and the irreversible change in action I , $\Delta I = l\Delta P_{\parallel}/k_{\parallel}$, which is the major contribution to energy diffusion, is determined by the phase (ζ in Eq 3.4). Very intense nonlinear whistlers, as observed recently on board Stereo satellite (Cattell *et al.*, 2008) may additionally enhance the initial energization (Omura *et al.*, 2008).

4. Implications

There may exist an interesting similarity in energization processes of electrons to (ultra) relativistic energies in a variety of vastly different magnetized plasmas. A common thread connecting these processes includes a strongly distorted large-scale magnetic field and a distant electron seed injection. In the discussed examples the large-scale magnetic fields exhibit the following distorted configurations: (a) terrestrial (planetary) magnetospheric field with a northward polarity is distorted due to a persistent southward interplanetary magnetic field; (b) solar coronal magnetic field is radically distorted when a large blob of plasma is detached from the corona and is propelled into the interplanetary medium as CME, preserving its magnetic connection to the solar surface; (c) strongly distorted magnetic field around accretion disc is frozen in the collimated jet plasma over vast spatial distances. In order for the proposed bootstrap mechanism to operate, an additional marginally stable, stressed magnetic field configuration is required: (i) pinching of the distant terrestrial magnetotail field and thinning of the supporting current results in a substorm, with a directly observed injection of nonisotropic, sub-relativistic electrons into closed terrestrial field lines; (ii) coronal field behind the propagating CME releases its tension via (indirectly deduced through 100s MHz emissions) injection of nonisotropic, sub-relativistic electrons into the closed coronal field lines; (iii) small-scale, inhomogeneous field arcs, required for consistency with observed synchrotron radiation emitted by the relativistic electrons in the galactic jets, reconnect and inject nonisotropic electrons into these closed field lines.

In all cases the injected electrons excite coherent whistler waves which propagate and reflect along the closed field lines, interacting efficiently with the tail of the electron population and boosting its energy to relativistic or ultra relativistic energies. Hence, the

bootstrap acceleration mechanism imposes several observational predictions: (a) the local enhancement of relativistic fluxes in the magnetospheric radiation belts will not be produced without bursty substorm injection, (b) the formation of the (delayed) heliospheric relativistic electrons will not occur without bursty coronal injection behind the intense propagating CME (which later opens the venue for the energetic electrons to the interplanetary medium); (c) the re-acceleration of the jet electrons would not occur via the bootstrap mechanism without formation of small-scale inhomogeneous magnetic fields. The energization time scale decreases dramatically with higher injected energy opening availability of additional resonant sites, and with a more anisotropic seed population resulting in higher whistler wave amplitudes.

References

- Baker, D., *et al.*, 1986, *Jour. Geoph. Res.*, **91**, 4265
 Blandford, R. D. & D. G. Payne, 1982 *MNRAS*, **199**, 883
 Bortnik, J., U. S. Inan, & T. F. Bell, 2006, *Geoph. Res. Lett.*, **33**, 3102
 Cattell, C. *et al.*, 2008, *Geoph. Res. Lett.*, **35**, L01105
 Fendt, C. & E. Memola, 2001, *Astronomy & Astrophysics*, **365**, 631.
 Fleishman, G. D., 2006, *Ap. Jour.*, 638, 348.
 Frederiksen, J. T. *et al.*, 2004, *Astrophys. J.*, **608**, L13
 Haggerty, D. K. *et al.*, 2003, *Adv. Space. Res.*, **32**, 2673
 Jester, S. *et al.*, 2004, *Astronomy & Astrophysics*, **431**, 477.
 Kimura, I., 1966, *Radio Sci.*, **1**, 269
 Kimura, I., 1985, *Space Sci. Rev.*, **42**, 449
 Klassen *et al.*, 2005, *Jour. Geoph. Res.*, **110**, AO9S04
 Krucker, S. *et al.*, 1999, *Astrophys. J.*, **519**, 864
 Lin, R. P., *Sol. Phys.*, **100**, 519, 1985.
 Maia, D. J. F. & M. Pick, *Astrophys. J.*, **609**, 1082, 2004.
 Medvedev, M. V., *Astrophys. J.*, **540**, 704, 2000.
 Meisenheimer, K. & A. F. Heavens., 1986, *Nature*, **323**, 419
 Meredith, N. *et al.*, *Geoph. Res. Lett.*, **30**, 1871, 2003.
 Nishikawa, 2005, *et al.*, *Astrophys. J.*, **622**, 927, 2005.
 Omura, Y., Y. Katoh, & D. Summers, *Jour. Geoph. Res.*, **113**, AO4223, 2008.
 Pick, M. & D. J. F. Maia, *Adv. Space Res*, **35**, 1876, 2005.
 Reeves, G. D., *et al.*, *Geoph. Res. Lett.*, **30**, 1529, 2003.
 Roth, I., M. Temerin, & M. K. Hudson, *Annales Geophysicae*, **17**, 631, 1999.
 Roth, I., *Jour. Atm. Sol. Terr. Phys.*, 70, 490, 2008.
 Shklyar, D. R., J. Chum, & F. Jiricek, *Ann. Geoph.*, **22**, 3589, 2004.
 Wang, L., R. P. Lin, S. Krucker, & J. T. Gosling, *Geoph. Res. Lett.*, **33**, L03106, 2006.

Discussion

THEJAPPA: In your picture, you show that type II emission is coming from quasiparallel shock and other emissions are coming from quasiperpendicular part of the shock in the downstream. How do you explain the electron acceleration by a quasiparallel shock and downstream near the flanks of such a shock?

ROTH: The type II low electron energy emissions are due to the propagating shock but the relativistic electrons are formed due to interaction with whistler waves, which are excited by the non-isotropic electrons, as observed by the NRH emissions, in resemblance to the magnetospheric observations.

SPANGLER: You mentioned the necessity of strong small-scale magnetic fields in extragalactic radio sources. Radio astronomical observations of such sources have given us much information on the magnetic field and energetic particles. The level that the synchrotron radiation is almost always polarized, and often highly polarized, places constraints on the amplitude and/or isotropy of small scale magnetic fluctuations.

ROTH: Several recent observations (Jester, 2005, and reference therein) eliminate the possibility of various electron sources, and the only possibility to explain the observed spectra asserts that small scale inhomogeneous magnetic field are crucial, and that their integrated energy density is of the order of the macroscopic magnetic energy density (Fleishman, 2005). The small scale features are very inhomogeneous. Polarization issue is not resolved yet experimentally.